Electrochemical synthesis of graphite-tetrafluoroaluminate intercalation compounds

Kazuhiko Matsumoto,* Kosuke Takagi, Rika Hagiwara[z,*]

Graduate School of Energy Science, Kyoto University, Yoshida Sakyo−ku, Kyoto 606−8501, Japan

* Electrochemical Society Active Member.

[z] Email: hagiwara@energy.kyoto−u.ac.jp, Tel: +81−75−753−5822, Fax: +81−75−753−5906

Abstract

Graphite tetrafluoroaluminate intercalation compounds (AlF_4-GICs) have been prepared by electrochemical oxidation of a natural graphite electrode in a 1.0 M nitromethane solution of tetraethylammmonium tetrafluoroaluminate ([TEA][AlF_4]). Galvanostatic electrolysis suggests that the intercalation reaction occurs above 0.8 V vs. Ag^+/Ag. Powder X-ray diffraction measurements of the AlF_4-GIC obtained by potentiostatic electrolysis reveal that the most AlF_4-rich phase is the stage-3 GIC with a gallery height of 0.79 nm. This gallery height agrees with the theoretical value calculated from the size of AlF_4^- that locates its two-fold axis perpendicular to the graphite layers. Co-intercalation of the solvent is suggested by the composition of the stage-3 GIC ($C_{55}AlF_4$) and is confirmed by release of the solvent above 350 K during thermogravimetric analysis. Although the AlF_4-GIC shows the higher air stability than those of the GICs with typical inorganic complex anions, it slowly decomposes into GICs at higher stages after exposure to the air over 1000 h. Increase of gallery height was observed during this period, which possibly results from reorientation of AlF_4^- between the layers. The thermodynamic stability of AlF_4-GIC is evaluated based on a Born-Harber cycle.

Introduction

Graphite intercalation compounds (GICs) were extensively studied by many chemists and physicists during the latter half of the last century due to their unique structural and electronic properties.[1-3] Since many compounds were found to exhibit electronic conductivities higher than that of the original graphite, they were called synthetic metals and their applications were envisaged as conductive materials lighter than metals. They are classified into two categories, donor- and accepter-types. The donor-type GICs are formed by reduction of the host graphite layers along with the intercalation of the guest species represented by alkali metal cations. The most successful application of GICs to date is actually not as electronic conductors but as the negative electrode of lithium ion batteries taking advantage of the reversible topotactic intercalation and deintercalation of lithium ion into and out of the host graphite.[4] The acceptor-type GICs are formed by oxidation of the graphite layers and intercalation of anionic guest species. The practical applicationsof the acceptor-type GICs has not been as successful as that of the donor-type GIC except for sulfate GIC as precursors for the preparation of exfoliated graphite.[5, 6]

Various fluoroanions are known to be intercalated into graphite, such as BF_4^-,[7-9] PF_6^-,[10, 11] AsF_6^-,[12] and SbF_6^-.[13] Even bulky anions with perfluoroorganic−group such as $PF_3(C_2F_5)_3$ and R_fSO_3 (R_f = long perfluoroorganic group) can be intercalated into graphite layers by significantly expanding the layer spacing.[4, 14, 15] The selection of the guest anion is an important factor to determine properties of acceptor-type GICs. Among a series of fluoroanions, the tetrafluoroaluminate anion (AlF_4^-) is one of the missing examples as a guest anion in GICs. The

AlF_4^- anion tends to form a polymeric structure and only a few salts with bulky organic cations contain the isolated tetrahedral AlF_4^- in both the solid and liquid states.[16-18] There are reports on the chemical reaction of AlF_3 and graphite in the presence of elemental fluorine.[19, 20] The product obtained by this reaction was not characterized as a GIC containing AlF_4^-, but was expressed as a GIC with a composition of $C_xF(AlF_3)_y$. This is in contrast to the well-known $AlCl_4$- and $AlBr_4$-GICs.[1]

This study reports the first synthesis of AlF_4−GIC by anodic oxidation of a graphite electrode in an organic medium containing AlF_4^-. The unique compound was characterized by means of X−ray diffraction and thermogravimetric analyses. The thermodynamic stability of AlF_4-GIC will be discussed using a Born-Haber cycle.

Experimental

General and Reagents. Air sensitive materials were handled in a glove box under a dried and deoxygenated argon atmosphere. Silver tetrafluoroborate (Wako Pure Chemical Industries, Ltd., Purity 97 %), tetraethylammonium tetrafluoroborate ([TEA][BF_4], Tokyo Chemical Industry Co., Ltd., purity > 98 %), [TEA]Cl (Tokyo Chemical Industry Co., Ltd., purity > 98.0 %), anhydrous $AlCl_3$ (Wako Pure Chemical Industries, Ltd., purity 99.9 %), acetonitrile (Wako Pure Chemical Industries, Ltd., water content ≤ 50 ppm), and nitromethane (Sigma-Aldrich Co., purity ≥ 98.5 %, water content ≤ 100 ppm), and SP-1 graphite powder (Union Carbide Corp., average particle diameter 100 μm, purity 99.4 %) were used as supplied. The starting material, [TEA][$AlCl_4$], was prepared by the equimolar reaction of $AlCl_3$ and [TEA]Cl in acetonitrile, followed by removal of

the solvent under vacuum at 343 K. Anhydrous HF (Stella Chemifa Corp., purity 99.9 %), was dried over K_2NiF_6 (Ozark−Mahoning Elf Atochem North America Inc.) prior to use (for treatment of anhydrous HF, see previous works[21,22]).

Synthesis of [TEA][AlF₄]. A large excess of anhydrous HF (aHF) was distilled onto 3.473 g of [TEA][$AlCl_4$] (1.161×10^{-2} mol) in a tetrafluoroethylene-perfluoroalkylvinylether copolymer (PFA) reactor at 77 K and the mixture was slowly warmed up to room temperature. The pressure inside the reactor rose due to evolution of HCl and the pressure of the reactor was carefully controlled by releasing the gas to the chemical trap. The temperature of the reactor was also controlled by an appropriate coolant. The byproduct HCl was pumped off together with excess HF at room temperature once the reaction ceased and a homogeneous liquid was obtained. Addition and elimination of aHF were repeated again to complete the reaction. The final product, [TEA][AlF_4], was obtained by evacuating the sample at 383 K for one day (2.707 g, 1.161×10^{-2} mol). Anal. Calcd. for $C_8H_{20}NF_4$: C, 41.20; H, 8.64; N, 6.01; F, 32.58. Found: C, 40.80; H, 8.68; N, 5.96; F, 32.86. IR (frequency/cm^{-1}): 785 (AlF_4^-).

Electrode preparation and electrochemical measurement. Graphite powder and KF polymer (Kureha Corp) were mixed in the 85:15 mass ratio of graphite and poly(vinylidene fluoride) (PVdF). This slurry was painted on a nickel mesh current collector (Nilaco Corp., 50 mesh) which was spot-welded to a nickel wire and electrochemically polished in sulfuric acid prior to use. The obtained electrode was dried under vacuum at 393 K for one day. The reference electrode was made by immersing a silver wire in a 0.01 M $AgBF_4$ + 0.1 M [TEA][BF_4] / CH_3NO_2 solution in a glass sample holder which was separated from the electrolytic solution by

porous Vycor glass (BAS Inc.). A counter electrode was prepared in the same manner as the working electrode and separated from the electrolytic solution by thin porous Vycor glass to minimize the effects of the product from the counter electrode. Electrochemical measurements were performed at 298 K with the aid of an electrochemical measurement system HZ−3000 (Hokuto Denko). The electrolytic solution was prepared by dissolving [TEA][AlF_4] into nitromethane (1 M).

Analysis. X-ray diffraction patterns were recorded by a powder X-ray diffractometer, Ultima IV (Rigaku Corp., CuKα radiation, 40 kV-40 mA). Air sensitive samples were placed in an air-tight cell with beryllium windows (Rigaku Corp.) under a dry argon atmosphere. Infrared spectra of [TEA][AlF_4] was obtained by using a FTS−155 spectrometer (Bio-Rad Laboratories Inc.). The sample compartment was filled with a dry argon gas during measurements. The samples were sandwiched between a pair of silver chloride windows in an air−tight cell under a dry argon atmosphere. Thermal decomposition behavior was analyzed by a differential thermogravimetric analyzer, DTG−60H (Shimadzu Corp.). Nickel cells were washed with acetone just before measurements and dried by heating. The measurement was performed at a scan rate of 5 K min^{-1} under the flow of dry argon gas (50 mL min^{-1}). The sample was heated from room temperature to 573 K and held there for 30 minutes. Elemental analysis was performed at the elemental analysis center in Institute for Chemical Research, Kyoto University.

Results and Discussion

Cyclic voltammetry and galvanostatic electrolysis. Figure 1 (a) shows the cyclic voltammogram

of a nickel plate in 1 M [TEA][AlF_4] / CH_3NO_2. During the anodic sweep, no obvious anodic current is observed due to passivation of the surface of the nickel electrode. A cathodic current ascribed to decomposition of the electrolytic solution is observed at –2.2 V vs. Ag^+/Ag during the cathodic sweep. A cyclic voltammogram of a graphite electrode in 1 M [TEA][AlF_4] / CH_3NO_2 is shown in Figure 1 (b). Anodic current is observed at 0.8 V vs. Ag^+/Ag during the anodic sweep, suggesting intercalation of AlF_4^- into graphite layers (eq. (1)). On reversing the sweep direction, a cathodic current corresponding to de-intercalation of AlF_4^- is observed.

$$x\mathrm{C} + \mathrm{AlF_4^-} \rightleftarrows \mathrm{C}_x\mathrm{AlF_4} + \mathrm{e} \qquad (1)$$

The value of Q_c/Q_a is 0.78, where Q_c and Q_a denote the cathodic and anodic charges in the cyclic voltammogram, respectively. This value indicates that a part of intercalated AlF_4^- remains in graphite layers after the cathodic sweep. The low Q_c/Q_a value is typical for the intercalation of inorganic complex anions such as BF_4^- and PF_6^- into graphite in nonaqueous electrolytes.[7, 8, 11, 23]

Figure 2 shows a galvanostatic charge profile of a graphite electrode in 1 M [TEA][AlF_4] / CH_3NO_2 at a current density of 10 mA g^{-1}. The profile shows a gentle gradient in the range of 0.8−1.2 V vs. Ag^+/Ag, which indicates phase transitions from the GIC with a higher stage number to that with the lower stage number. Above 1.2 V vs. Ag^+/Ag, the potential increased steeply, suggesting oxidation of the lowest-stage GIC or anodic decomposition of the electrolyte on the GIC.

Potentiostatic electrolysis. Figure 3 shows a chronoamperogram of a graphite electrode in 1 M [TEA][AlF_4] / CH_3NO_2 during potentiostatic electrolysis at 1.1 V vs. Ag^+/Ag. The current density

decreased with an increase in electrolysis time and the total charge reached 168 C g^{-1} at 1800 s. This charge density corresponds to the composition of $C_{48}AlF_4$.

An XRD profile of the electrode after the potentiostatic electrolysis (without washing) is shown in Figure 4. Structural parameters obtained from this XRD pattern are listed in Table 1. This GIC can be indexed as a stage-3 compound (n = 3) according to the following eq. (2):

$$(n + 1)d_{00n+1} = (n + 2)d_{00n+2} (= I_c) \quad (2)$$

Where n and I_c denote the stage number and the unit cell repeat length (identity period) along the stacking direction, respectively.

The resulting gallery height (d_i) is in the range of 0.79−0.80 nm; the value calculated from the (001) diffraction peak contains a large experimental error. The d_i value obtained from the most intense (004) diffraction peak is 0.795 and agrees with the calculated value of 0.791 nm based on the model where AlF_4^- locates the two-fold axis perpendicular to the graphite layers as shown in Figure 5 (a) (see crystallographic data of [collidineH^+][AlF_4^-] which gives the average Al–F bond of 0.165 nm for the tetrahedral AlF_4^- [13])[17]. This gallery height is slightly larger than that of BF_4-GIC (0.749 nm) with the same orientation in the graphite layers,[9] as is expected from the sizes and geometry of AlF_4^- and BF_4^-. Although potentiostatic electrolysis at higher potentials was attempted, an AlF_4–GIC at lower stage (stage-1 or stage-2 GICs) was not obtained.

The compositions of the obtained GICs ($C_{48}AlF_4$ at 1.1 V) suggest co-intercalation of the solvent nitromethane since the ratio of AlF_4^- to carbon is less than that usually obtained for a

stage-3 compound (see the case of BF_4-GIC with a composition around $C_{20}BF_4$ for a stage-3 compound without co-intercalation).[9] Similar phenomena were observed for GICs of other anions prepared in organic solutions.[24, 25] The thermogravimetric curve of the stage-3 AlF_4-GIC is shown in Figure 6 with that of PVdF for comparison. The stage-3 AlF_4-GIC steeply loses its weight from 350 K and reaches 94 % of its original weight at 570 K. The weight loss suggests that the amount of nitromethane (k) co-intercalated with AlF_4^- is more than 0.71 in the formula of $C_{48}AlF_4(CH_3NO_2)_k$. It should be noted that the thickness of nitromethane is small enough to be co-intercalated into the graphite layer without affecting the gallery height when its long axis is parallel to the graphite layer (cf. the crystallographically determined structure of nitromethane[26]).

Air stability and structural change. The air stability of the stage-3 AlF_4-GIC was investigated by periodic XRD measurements. The sample was prepared by potentiostatic electrolysis at 1.1 V vs. Ag^+/Ag as shown above. Figure 7 shows the change in XRD profiles of the electrochemically prepared GIC during exposure to the air at room temperature. The diffraction peaks are broadened with exposure time and formation of the higher stage GIC is suggested. It should be noted that both the (004) and (005) peaks shifted to lower angles during the first week (from 24.3° to 24.0° for the (004) peak and from 30.4° to 29.7° for the (005) peak), suggesting an increase in d_i. The peak at 24.0° does not shift during further exposure to the air, whereas the peak at 29.7° shifted to the low angle (29.4° after three weeks and 28.9° after six weeks).

Although the diffraction patterns of the GICs after one week and three weeks are unindexable probably due to the formation of complicated solid solutions, the pattern obtained

after six weeks in air is indexable as a stage-4 GIC with d_i of 0.845 nm (2θ = 24.1° and d = 0.369 nm for (005) and 2θ = 28.9° and d = 0.309 nm for (006)) using eq. (2). The asymmetric shapes of these peaks suggest stage mixing or formation of solid solutions in these materials. One possible structural change during this period is reorientation of AlF_4^- within the layer; the three-fold axis of AlF_4^- lies perpendicular to the graphite layers with a theoretical d_i of 0.821 nm (Figure 5 (b), see the other case above (the two−fold axis perpendicular to the graphite layers) for calculation of d_i). Another possibility is formation of a polymeric or oligomeric fluoroaluminate anion in the layer.[27, 28] Although the infinite chains consisting of AlF_6 octahedra which are corner-shared to two pairs of edge-shared octahedra was reported as one of the polymeric units of AlF_4^-, this model leads to d_i larger than 0.952 nm (this value is obtained in the case when the *trans* F−Al−F axis in a AlF_6 unit with the Al−F length of 0.176 nm lies perpendicular to the graphite layers) and is therefore excluded in the present case. The ladder−like $(Al_2F_8^{2-})_n$ chain is another possible structural motif in graphite layers (Figure 5 (c)). In this case, the smallest d_i of 0.869 nm is based on the F···F distance (0.268 nm) between the two terminal fluorine atoms (*cis*−F−Al−F relation to each other) when the slightly zig-zag configuration of the AlF_6 octahedron is ignored. This value is still too large compared to the observed 0.845 nm for the stage-4 compound obtained after six-week exposure to the air. Consequently, the formation of a polymeric unit does not seem to occur in this case. The uptake of water from the air is another possible factor to contribute to the increase of d_i, because AlF_4^- can transform to water−containing species, $AlF_4(H_2O)_l^-$.[27, 29, 30] However, considering the high oxidation power of fluoroanion-GICs, this is not very plausible.

Lerner and his co−workers reported that GICs with large anions such as $N(SO_2CF_3)_2^-$ are

more stable in air than those of the GICs with small inorganic anions (NO_3^-, SO_4^{2-}, and FHF^-).[31] They proposed that the reason for this phenomenon is the slow diffusion rate of the large guest species in GICs. Although the size of AlF_4^- is similar to the small inorganic anions indicated, the increase in stage number for the present AlF_4-GIC is slower than those with NO_3^-, SO_4^{2-}, and FHF^-. The fairly stable Al−F bond may maintain the structure of the AlF_4-GIC around stage-4 even after exposure to the air over 1000 h.

Thermodynamic stability of AlF_4−GIC.

As was pointed out by Bartlett and his co-workers, the majority of fluoroanions (from tetrahedral BF_4^- to octahedral UF_6^-) have approximately the same effective ionic diameter of roughly 0.50 nm when they are guests in graphite.[2, 32-34] Application of a modified Born-Haber cycle to such acceptor-type GICs of fluorometallate anions based on an ionic model shows that the thermodynamic requirement for GIC formation is predominantly governed by the formation enthalpy of fluorometallate anions from molecular fluorides (eq. 3).[34, 35]

$$MF_{n(g)} + 1/2F_{2(g)} + e \rightarrow MF_{n+1}^-{}_{(g)} \quad (3)$$

From a series of experiments, they determined the threshold enthalpy range of this process for the intercalation into graphite to be −440 ~ −520 kJ mol^{-1}. Partial intercalation, namely the formation of high stage salts, occurs in this range. When the enthalpy is lower than −520 kJ mol^{-1}, full intercalation, i.e. formation of the 1st stage salt, occurs, whereas no intercalation proceeds

when it is higher than −440 kJ mol^{-1}. The reaction step given in eq. 3 can be divided into two processes:

$$1/2F_{2(g)} + e \rightarrow F^-_{(g)} \quad (4)$$

$$MF_{n(g)} + F^-_{(g)} \rightarrow MF_{n+1}{}^-_{(g)} \quad (5)$$

The enthalpy change for the process given by eq. 4 is estimated to be −256 kJ mol^{-1}.[36] The enthalpy change for the process given by eq. 5 is defined as fluoride ion affinity of the Lewis acid fluorides. Thus, the threshold enthalpy change for graphite intercalation is −180 ~−260 kJ mol^{-1} in terms of fluoride ion affinity.

The fluoride ion affinity of AlF_3 has been evaluated by several groups (e.g. −548 kJ mol^{-1}).[37] This value indicates that the formation of the 1st stage salt is thermochemically allowed. However, under ambient conditions, AlF_3 is a stable solid and gasification enthalpy (301 kJ mol^{-1})[38] should be taken account when the reaction starts from solid AlF_3 (eq. 6).

$$AlF_3(s) \rightarrow AlF_3(g) \quad (6)$$

Therefore, the enthalpy change for the process given by eq. 7 is −247 kJ mol^{-1} that falls in the range for the formation of high stage GIC.[34, 35]

$AlF_{3(s)} + 1/2F_{2(g)} + e \rightarrow \quad AlF_4^-{}_{(g)}$ (7)

The large gasification energy of AlF_3 leads to the difficulty in synthesizing AlF_4-GIC from AlF_3, whereas the electrochemical synthesis using a soluble salt as an AlF_4^- source is an effective method because it directly intercalates AlF_4^- into the graphite layers. Although a GIC at a lower stage than expected by the Born-Haber cycle may be prepared when a solvent is co-intercalated, the present study confirmed only the stage-3 GIC by the electrochemical method.

Conclusion

This study reports the first synthesis of AlF_4-GIC by an electrochemical method. Cyclic voltammetry confirms intercalation of AlF_4^- into the graphite structure occurs above 0.8 V vs. Ag^+/Ag during the anodic scan, whereas the deintercalation does not fully occur during the following cathodic scan. Galvanostatic electrolysis showed a gradual staging reaction in the range of 0.8−1.2 V vs. Ag^+/Ag. Potentiostatic electrolysis at 1.1 V vs. Ag^+/Ag combined with XRD reveals that the GIC reached stage-3 but the lower stage GIC was not obtained. The gallery height suggests that AlF_4^- is oriented with its two-fold axis perpendicular to the graphite layers just after the synthesis. Exposure to the air of the AlF_4-GIC results in a change in the gallery height, which may be caused by the change in the orientation of AlF_4^- (the three-fold axis perpendicular to the graphite layers). Thermodynamic evaluation using a Born-Haber cycle agrees with the stability of a AlF_4-GIC forms a high-stage structure rather than a stage-one structure.

Table 1 Structural parameters obtained from the XRD profile of the stage-3 GIC obtained by potentiostatic electrolysis of a graphite electrode at 1.1 V vs. Ag^+/Ag in 1 M [TEA][AlF_4] / CH_3NO_2

hkl	2θ / degree	*d* / nm	I_c / nm	d_i / nm
001	5.95	1.49[a]	1.49[a]	0.82[a]
004	24.3	0.366	1.465	0.795
005	30.4	0.294	1.469	0.799
–	42.4	0.213	–	–
–	44.2	0.205	–	–
008	49.9	0.183	1.462	0.792
009	56.4	0.163	1.466	0.796

[a]These values contain large experimental errors from the low 2θ angle and weak intensity.

Figure captions

Figure 1 Cyclic voltammograms of (a) a nickel electrode and (b) a graphite electrode in 1 M [TEA][AlF_4] / CH_3NO_2.

Figure 2 A galvanostatic charge profile of a graphite electrode in 1 M [TEA][AlF_4] / CH_3NO_2.

Figure 3 A chronoamperogram of a graphite electrode in 1 M [TEA][AlF_4] / CH_3NO_2 during potentiostatic electrolysis at 1.1 V vs. Ag^+/Ag.

Figure 4 An X-ray diffraction profile of the graphite electrode obtained by potentiostatic electrolysis at 1.1 V vs. Ag^+/Ag in 1 M [TEA][AlF_4] / CH_3NO_2. The symbol ♦ denotes the strongest diffraction peak of [TEA][AlF_4].

Figure 5 (Color online) A possible alignment of AlF_4^- in graphite layers; (a) the discrete AlF_4^- with the C_{2v} axis perpendicular to the graphite layers, (b) the discrete AlF_4^- with the C_{3v} axis perpendicular to the graphite layers, and (c) the ladder-like $(Al_2F_8^{2-})_n$ chain. The *c*-axis in the diagrams denotes the direction perpendicular to the graphite layers.

Figure 6 Thermogravimetric curves for PVdF and the stage-3 AlF_4-GIC.

Figure 7 X-ray diffraction patterns of the stage-3 AlF_4-GIC obtained by potentiostatic electrolysis at 1.1 V vs. Ag^+/Ag in 1 M [TEA][AlF_4] / CH_3NO_2 during exposure to the air at room temperature.

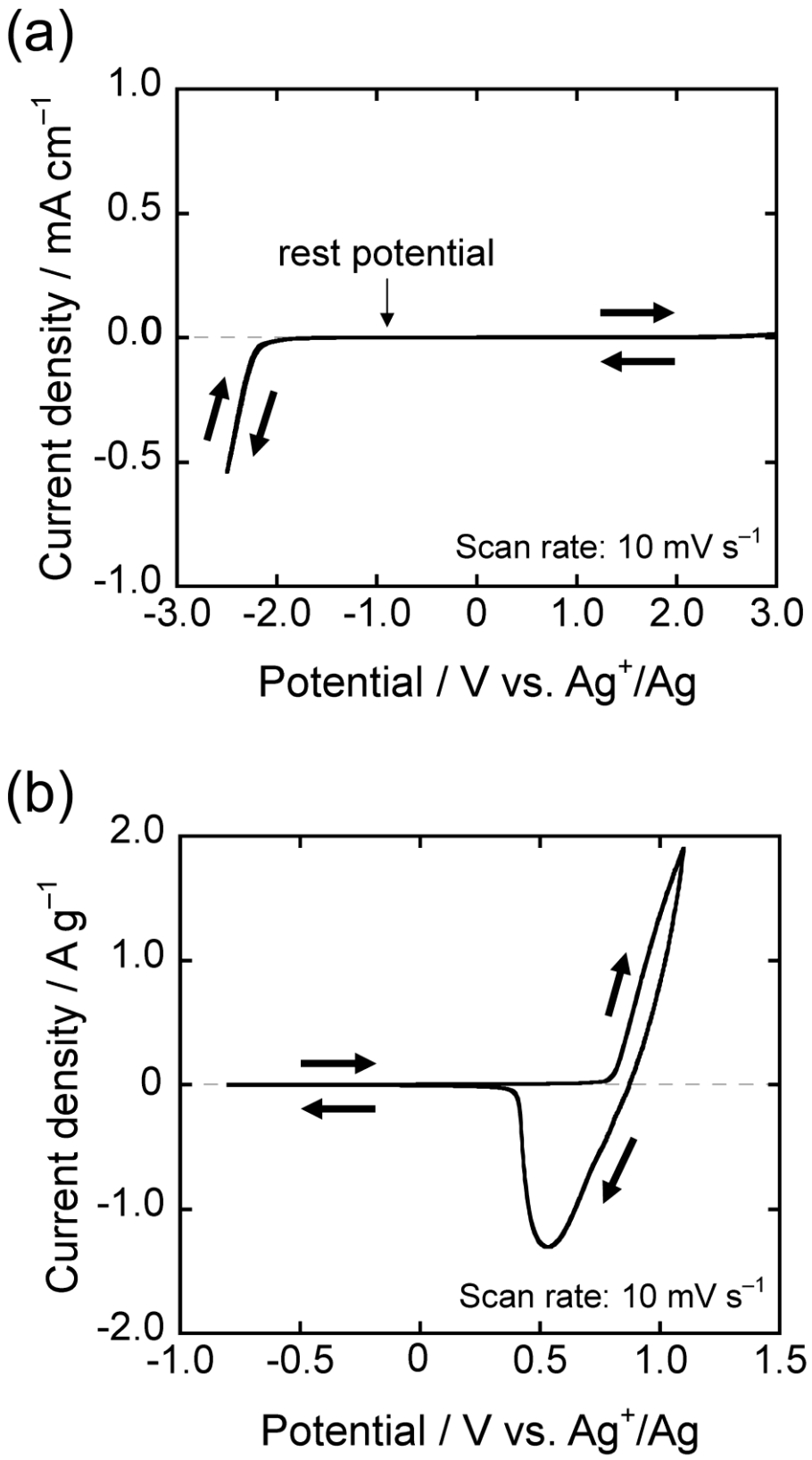

Figure 1 Cyclic voltammograms of (a) a nickel electrode and (b) a graphite electrode in 1 M [TEA][AlF_4] / CH_3NO_2.

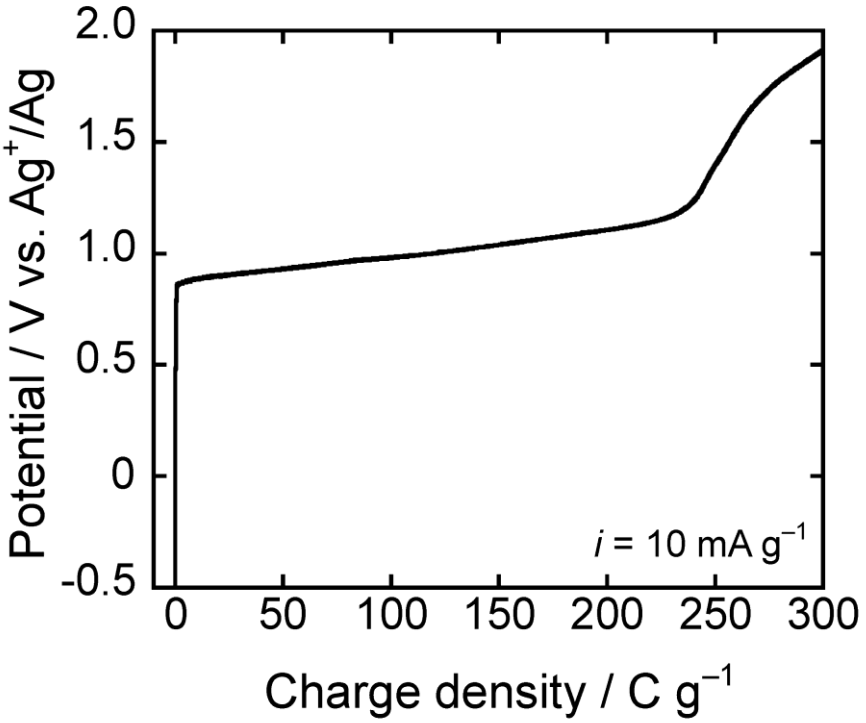

Figure 2 A galvanostatic charge profile of a graphite electrode in 1 M [TEA][AlF_4] / CH_3NO_2.

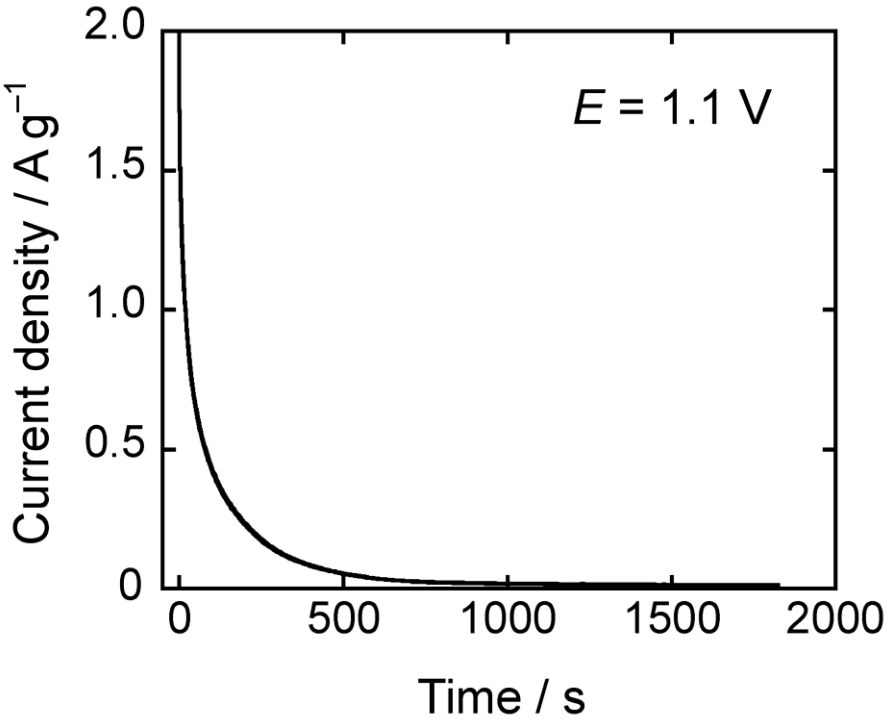

Figure 3 A chronoamperogram of a graphite electrode in 1 M [TEA][AlF_4] / CH_3NO_2 during potentiostatic electrolysis at 1.1 V vs. Ag^+/Ag.

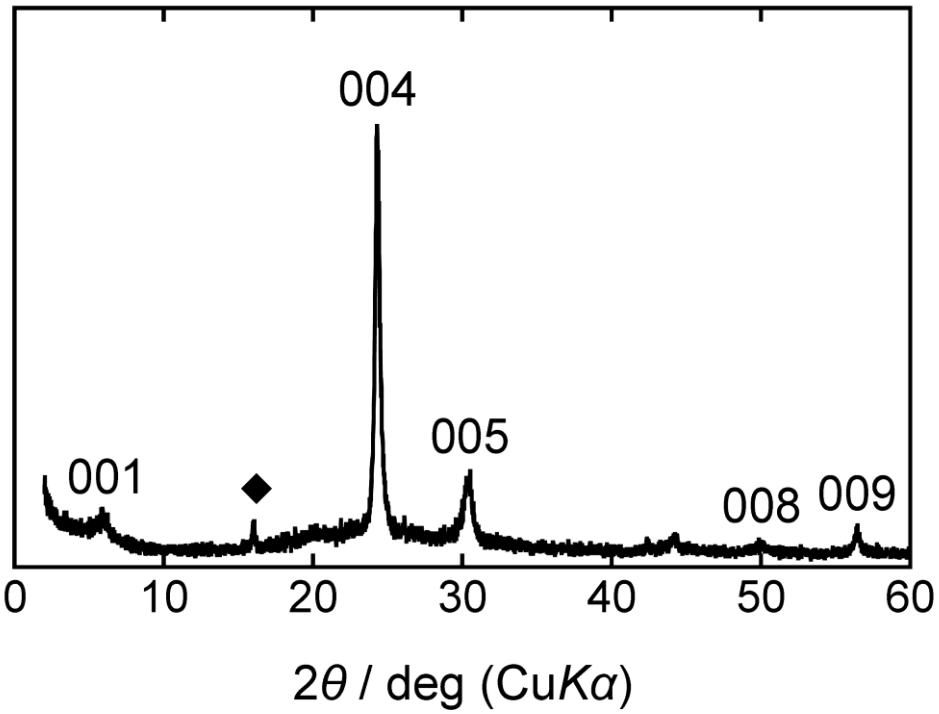

Figure 4 An X-ray diffraction profile of the graphite electrode obtained by potentiostatic electrolysis at 1.1 V vs. Ag^{+}/Ag in 1 M [TEA][AlF_4] / CH_3NO_2. The symbol ♦ denotes the strongest diffraction peak of [TEA][AlF_4].

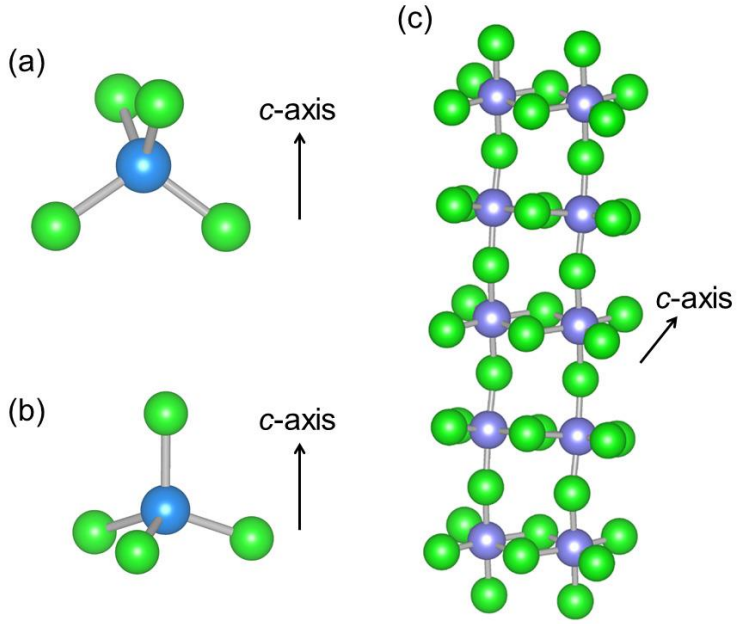

Figure 5 (Color online) A possible alignment of AlF_4^- in graphite layers; (a) the discrete AlF_4^- with the C_{2v} axis perpendicular to the graphite layers, (b) the discrete AlF_4^- with the C_{3v} axis perpendicular to the graphite layers, and (c) the ladder-like $(Al_2F_8^{2-})_n$ chain. The *c*-axis in the diagrams denotes the direction perpendicular to the graphite layers.

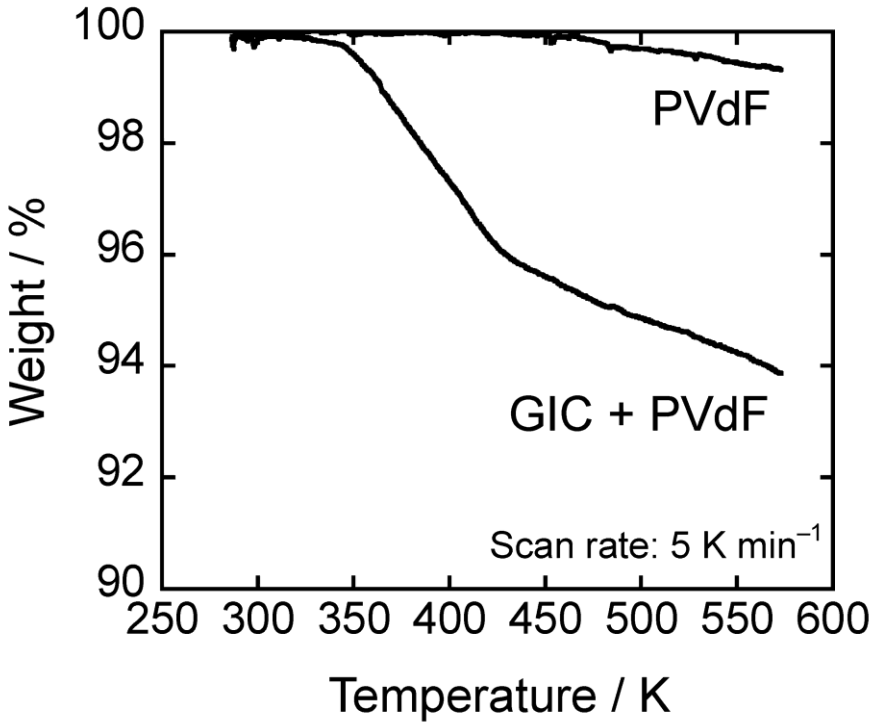

Figure 6 Thermogravimetric curves for PVdF and the stage-3 AlF_4-GIC.

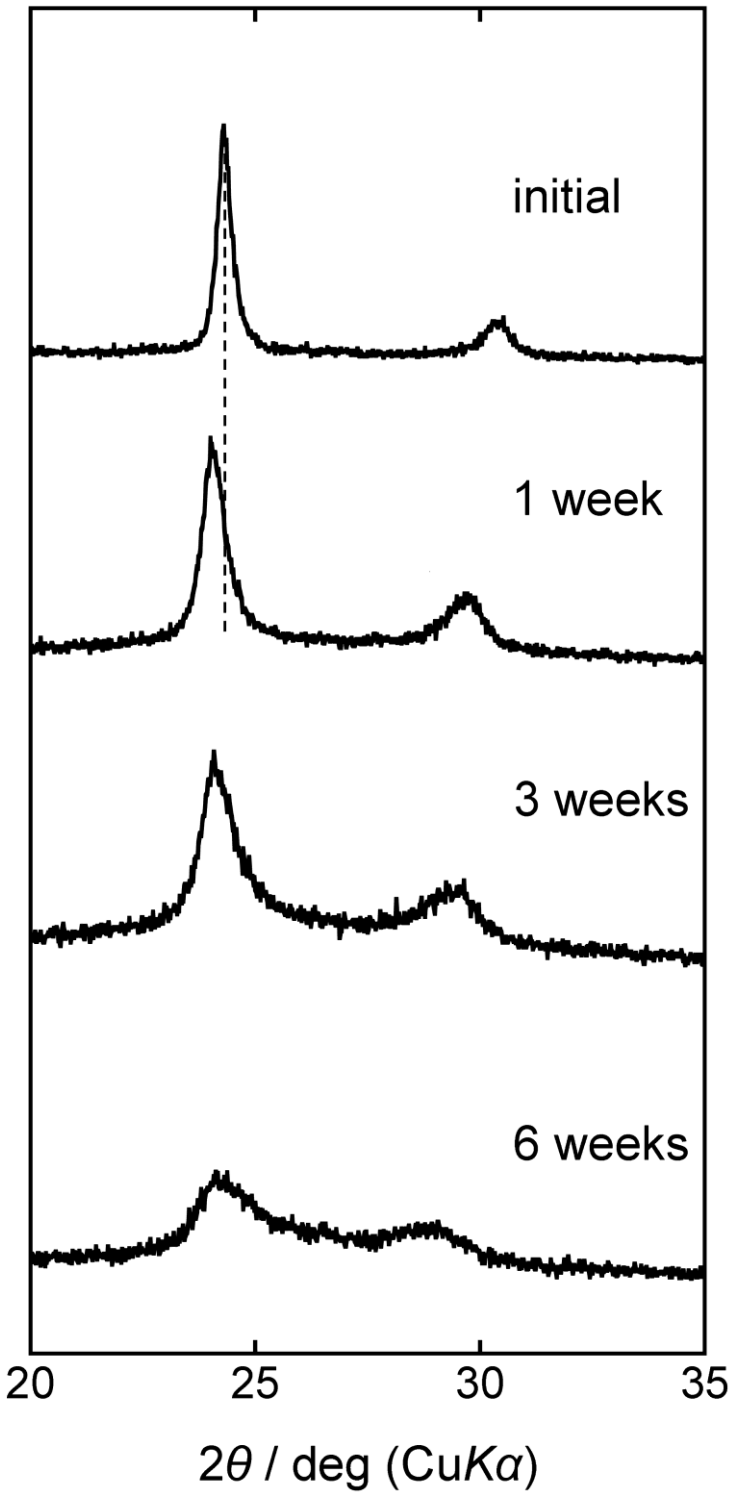

Figure 7 X-ray diffraction patterns of the stage-3 AlF_4-GIC obtained by potentiostatic electrolysis at 1.1 V vs. Ag^+/Ag in 1 M [TEA][AlF_4] / CH_3NO_2 during exposure to the air at room temperature.

References

1 M. S. Dresselhaus and G. Dresselhaus, *Adv. Phys.*, **30**, 139 (1981).

2 N. Bartlett and B. W. McQuillan, *Graphite Chemistry*, in *Intercalation Chemistry*, edited by e. S. M. Whittingham and A. J. Jacobsen, Academic Press, New York, 1982, p. 19.

3 H. Selig and L. B. Ebert, *Adv. Inorg. Chem. Radiochem.*, **23**, 281 (1980).

4 M. Noel and R. Santhanam, *J. Power Sources*, **72**, 53 (1998).

5 D. D. L. Chung, *J. Mater. Sci.*, **22**, 4190 (1987).

6 A. Celzard, J. F. Mareche, and G. Furdin, *Prog. Mater. Sci.*, **50**, 93 (2005).

7 P. W. Ruch, M. Hahn, F. Rosciano, A. Holzapfel, H. Kaiser, W. Scheifele, B. Schmitt, P. Novak, R. Kotz, and A. Wokaun, *Electrochim. Acta*, **53**, 1074 (2007).

8 Y. Yokoyama, N. Shimosaka, H. Matsumoto, M. Yoshio, and T. Ishiharaa, *Electrochem. Solid-State Lett.*, **11**, A72 (2008).

9 H. Selig and D. Brusilovsky, *J. Fluorine Chem.*, **57**, 15 (1992).

10 Z. Zhang and M. M. Lerner, *J. Electrochem. Soc.*, **140**, 742 (1993).

11 T. Ishihara, M. Koga, H. Matsumoto, and M. Yoshio, *Electrochem. Solid-State Lett.*, **10**, A74 (2007).

12 F. Okino, *J. Fluorine Chem.*, **105**, 239 (2000).

13 S. Karunanithy and F. Aubke, *J. Fluorine Chem.*, **23**, 541 (1983).

14 B. Ozmen-Monkul and M. M. Lerner, *Carbon*, **48**, 3205 (2010).

15 W. Yan and M. M. Lerner, *Carbon*, **42**, 2981 (2004).

16 N. Herron, R. L. Harlow, and D. L. Thorn, *Inorg. Chem.*, **32**, 2985 (1993).

17 N. Herron, D. L. Thorn, R. L. Harlow, and F. Davidson, *J. Am. Chem. Soc.*, **115**, 3028 (1993).

18 M. Ferbinteanu, H. W. Roesky, F. Cimpoesu, M. Atanasov, S. Kopke, and R. Herbst-Irmer, *Inorg. Chem.*, **40**, 4947 (2001).

19 T. Nakajima, M. Kawaguchi, and N. Watanabe, *Chem. Lett.*, 1045 (1981).

20 T. Nakajima, M. Kawaguchi, and N. Watanabe, *Z. Naturforsch B*, **36**, 1419 (1981).

21 K. Matsumoto and R. Hagiwara, *J. Fluorine Chem.*, **131**, 805 (2011).

22 D. Peters and R. Miethchen, *J. Fluorine Chem.*, **79**, 161 (1996).

23 R. T. Carlin, H. C. Delong, J. Fuller, and P. C. Trulove, *J. Electrochem. Soc.*, **141**, L73 (1994).

24 A. Jobert, P. Touzain, and L. Bonnetain, *Carbon*, **19**, 193 (1981).

25 G. R. Miller, H. A. Resing, M. J. Moran, L. Banks, F. L. Vogel, A. Pron, and D. Billaud, *Synth. Met.*, **8**, 77 (1983).

26 I. Y. Bagryanskaya and Y. V. Gatilov, *J. Struct. Chem.*, **24**, 150 (1983).

27 U. Bentrup, M. Feist, and E. Kemnitz, *Prog. Solid State Chem.*, **27**, 75 (1999).

28 K. Adil, M. Leblanc, V. Maisonneuve, and P. Lightfoot, *Dalton Trans.*, **39**, 5983 (2010).

29 U. Bentrup and W. Massa, *Z. Anorg. Allg. Chem.*, **593**, 207 (1991).

30 O. Knop, T. S. Cameron, S. P. Deraniyagala, and D. Adhikesavalu, *Can J Chem*, **63**, 516 (1985).

31 X. Zhang, M. M. Lerner, H. Gotoh, and M. Kawaguchi, *Carbon*, **38**, 1775 (2000).

32 N. Watanabe, H. Touhara, T. Nakajima, N. Bartlett, T. Mallouk, and H. Selig, *Fluorine Intercalation Compounds of Graphite*, in *Inorganic Solid Fluorides*, edited by P. Hagenmuller, Academic Press, New York 1985, p. 331.

33 N. Bartlett, F. Okino, T. E. Mallouk, R. Hagiwara, M. Lerner, G. L. Rosental, and K. Kourtakis, *Oxidative Intercalation of Graphite by Fluoronanionic Species*, in *Advances in Chemistry Series No. 226, Electron Transfer in Biology and the solid State: Inorganic Compounds with Unusual Properties*, edited by M. K. Johnson, R. B. King, D. M. Kurtz, C. Kutal Jr., M. L. Norton and R. A. Scott, American Chemcial Society, Washington, D. C., 1990., p. 391.

34 M. Lerner, R. Hagiwara, and N. Bartlett, *J. Fluorine Chem.*, **57**, 1 (1992).

35 R. Hagiwara and N. Bartlett, *Thermodynamic Aspects of the Intercalation of Graphite by Fluoroanions*, in *Fluorine-Carbon and Fluoride-Carbon Materials* edited by T. Nakajima, Marcel Dekker, Inc. , New York, 1995, p. 67.

36 D. D. Wagman, W. H. Evans, V. B. Parker, R. H. Schumm, S. M. Bailey, I. Hallow, K. L. Churney, and R. L. Nuttall, *Selected Values of Chemical Thermodynamic Properties*, in *National Bureau of Standards Technical Notes 270-3, 270-4, 270-5, 270-6, 270-7 and 270-8, Handbook of Chemistry and Physics, Vol. 70*, CRC Press, Boca Raton, FL,, 1989-1990.

37 J. L. Holm, *Acta Chem. Scand.*, **27**, 1410 (1973).

38 *JANAF Thermodynamical Tables,1971*. Clearinghouse for Federal Scientific and Technical Information, Springfield, Va. , 1971.